

Static and Dynamic Behaviors of Detached Plasmas in Divertor Simulator NAGDIS-II

TAKAMURA S.* , OHNO N., UESUGI Y.¹, NISHIJIMA D., OHSUMI K., MOTOYAMA M.,
HATTORI N., EZUMI N.², KRASHENINNIKOV S.³, PIGAROV A.³ and WENZEL U.⁴

Department of Energy Engineering and Science, Graduate School of Engineering,

¹*Center for Integrated Research in Science and Engineering, Nagoya University, Nagoya 464-8603, Japan*

²*Nagano National College of Technology, Nagano 381-8550, Japan*

³*University of California at San Diego, La Jolla, California 92093-0411, USA*

⁴*Max-Planck-Institut für Plasmaphysik, EURATOM Association, D-1011 Berlin, Germany*

(Received: 5 December 2000 / Accepted: 18 August 2001)

Abstract

Comprehensive investigations on the stationary behaviors in detached recombining plasmas in the linear divertor plasma simulator, NAGDIS-II, are summarized in relation to the phenomena observed in tokamaks with magnetic divertor. Structural dynamics due to injection of ELM-like plasma heat pulse produced by whistler wave heating into the detached helium plasma have been clarified in terms of quenching of plasma recombination, transport of plasma heat and particles, and recovery of recombination. Several time scales and specific energies are proposed to characterize the impact of ELM on the detached recombining plasmas and to understand the underlying physics. The identification of origin of the so-called inverse ELM and the role of highly excited Rydberg atoms are summarized.

Keywords:

structural dynamics, plasma detachment, recombining plasma, edge localized mode, divertor

1. Introduction

The plasma detachment is a key concept to solve heat and particle control in magnetically confined fusion experimental reactors. It should be realized together with a good core confinement. The ELM (Edge Localized Mode) heat pulse associated with the good confinement should be tolerable in terms of critical pulse energy depending on the target material. Compatibility of plasma detachment with the good confinement of high density plasma and a mitigation of ELM energy deposition is one of urgent issues to solve for a future successful realization of fusion experimental reactors [1].

The divertor plasma simulator NAGDIS-II has been providing a lot of basic knowledge concerning the

stationary characteristics of plasma detachment [2-11]. Recently, we are focusing our research on the dynamic behaviors of detached recombining plasmas against ELM-like plasma heat pulses generated by radio-frequency plasma heating [12,13], in which the transitions from detached to attached plasma or from recombining to ionizing plasmas and vice versa have been identified. Enhanced ionization of highly excited atoms generated by plasma recombination was found to make a prompt ion flux to the target. The so-called inverse ELM observed in diverted tokamaks was explained with collisional radiative atomic model of recombining as well as ionizing plasmas.

In this work, we would like to focus on the detailed

*Corresponding author's e-mail: takamura@nuee.nagoya-u.ac.jp

description of what is going on when injecting ELM-like heat pulse into the detached recombining plasmas. Especially, structural dynamics along the magnetic field line is the main concern in terms of quenching of plasma recombination, transport of plasma heat and particles to the target and recovery of recombination. Several time scales and characteristic energies are proposed to characterize the ELM impacts on the detached recombining plasmas. They are also keys to understand the underlying physics. The interesting response against a train of many short pulses is also represented.

2. Stationary Behaviors

The NAGDIS-II device [2-13] shown schematically in Fig. 1 has a vacuum chamber of 2.5 m in length and 0.18 m in diameter with the magnetic field intensity up to 2.5 kG. The neutral gas pressure in the plasma test region can be controlled from 1 to 30 mtorr to realize attached as well as detached plasmas by feeding a secondary gas and/or changing the pumping speed near the target plate. Fast scanning probes to measure the plasma parameters are installed at $X = 0.25$ m (entrance), 1.06 m (upstream), 1.39 m (midstream) and 1.72 m (downstream) from the plasma emanating anode with its aperture of 24 mm in diameter. The ion flux under only detached conditions and the floating voltage are measured at the target plate located at $X = 2.05$ m. Spectra of light emissions are detected at the above three locations. This device can generate high density plasma n_e up to 10^{20} m^{-3} for He and 10^{19} m^{-3} for H in steady state relevant to the divertor plasmas in fusion devices. The electron temperature T_e is ranged from 5 to 10 eV.

The discharge current of 80 A produces He plasma with $n_e = 4.0 \times 10^{19} \text{ m}^{-3}$ and $T_e = 8.5 \text{ eV}$ at the entrance. At an increased He neutral pressure P_{He} of 6.5 mtorr, the plasma detachment just starts. In the pure He plasmas, a minimum density to have a detachment is identified [3]

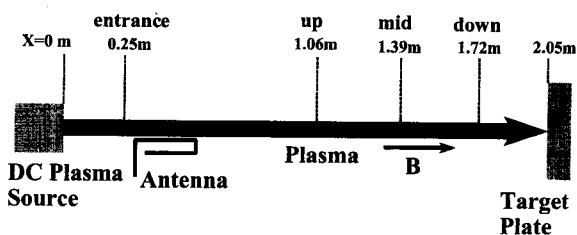


Fig. 1 Schematic configuration of divertor simulator NAGDIS-II.

because the electron-ion energy coupling is essential for the electron cooling since the ion energy is lost through charge exchange with neutrals. Such a density threshold was confirmed by using 2-D fluid B2 code to calculate the field aligned structure [2]. A strong anomaly of single Langmuir probe characteristics observed in detached low-temperature plasmas was reported to give us a considerably high T_e compared with the value determined spectroscopically. The reason has been discussed in terms of T_e gradient along the B field associated with the parallel electron transport [5]. Detailed evaluation of T_e and n_e of detached recombining plasmas by two different spectroscopic methods, using continuum emission and a series of line emission from highly excited levels was carried out, showing a typical roll-over of n_e with increase in gas pressure and a subsequent decrease, observed in divertor plasmas of tokamaks [11]. The different evaluation of T_e was discussed based on the presence of energetic electrons. All the above studies concern the plasma detachment due to electron-ion recombination (EIR) including three-body and radiative recombinations.

Another recombination process associated with molecular reactions, that is, molecular activated recombination (MAR) involving a vibrationally excited hydrogen molecule such as $\text{H}_2(v) + e \rightarrow \text{H}^- + \text{H}$ followed by $\text{H}^- + \text{A}^+ \rightarrow \text{H} + \text{A}$, and $\text{H}_2(v) + \text{A}^+ \rightarrow (\text{AH})^+ + \text{H}$ followed by $(\text{AH})^+ + e \rightarrow \text{A} + \text{H}$, where A^+ and A are the hydrogen helium or other impurity ion and atom, respectively existing in divertor plasmas, was pointed out in theory and modelling [14-16]. MAR was clearly observed for the first time in NAGDIS-II [6]. Hydrogen gas puffing into a He plasma strongly reduced the ion flux along the B field, although the conventional EIR was quenched. Careful comparison of the observed He Balmer spectra with collisional radiative (CR) atomic molecular data indicates that the enhanced population distribution over the atomic levels with relatively low principal quantum numbers can be well explained by taking the MAR into account. Structural difference of detached plasma between EIR and MAR was identified in the modelling [4,7] and experiment [8] in helium/hydrogen mixture plasmas. MAR in pure hydrogen plasma was discussed for a necessary plasma condition to obtain plasma detachment through MAR or EIR in tokamak divertor conditions [10].

Recent experiments show a coexistence of He and hydrogen Balmer series spectra indicating EIR root when a small amount of H_2 gas was introduced into the He plasma [17,18]. When more H_2 gas is introduced and

the partial hydrogen gas pressure exceeds a critical level, both continuum and series of line emission disappear, that is, EIR does not occur at all in the plasma, suggesting a transition to MAR [6]. Therefore, we can identify the boundary for EIR-MAR transition in the parameter space of He plasma density and H₂ gas injection rate.

3. Dynamic Behavior of Plasma Detachment

3.1 Background

First of all, we remind you the importance of ELM-like heat pulse in view of the erosion of divertor target plate in steady state fusion experimental reactor. Figure 2 shows a schematic of the ELM energy transport through SOL (Scrape-off Layer) and detached recombining plasma onto the divertor target plate. There have been strong worries about the tolerance of ELM energy into the divertor plate made of graphite or tungsten [19]. We have to know what happens in the ELM transport through SOL and divertor plasma. Time-dependent analysis with proper atomic physics is necessary, taking conductive and convective transport into account.

3.2 Generation of Heat Pulse

The rf heating has been employed to generate the electron heat pulse. The antenna consists of 25 cm × 2 folded bar along the magnetic field, driven with the frequency of 13.56 MHz located between ion and electron cyclotron frequencies, corresponding to the frequency range of whistler wave. Figure 1 gives a schematic of experimental configuration. Figure 3(a) shows the results of B2 fluid simulation on the field-aligned structure of He plasma density n_e and temperature T_e . The e-i collisional damping of the wave is so strong as shown in Fig. 3(b) that the wave energy may be completely absorbed in a very low temperature high-density recombining plasma. Some direct acceleration of electrons by the antenna near field along the magnetic field would have an effect on the phenomena.

The employed heat pulse may have a very similar character to the real ELM heat pulse coming from the electron heat conduction rather than the convection of plasma through SOL.

3.3 Categorization of Heat Pulse

Here we would try to give a categorization of ELM according to the pulse duration time and the total energy, as shown in Table I. We define the basic

parameters as follows: τ_{ELM} is the ELM pulse duration; $\tau_{\text{CONV}} = L/(\alpha C_S)$ or L^2/D where $\alpha \sim 0.2$ is the convection time for the upstream plasma to flow into the recombining region with the characteristic scale of L , C_S is the sound speed and D is the parallel diffusion coefficient. E_{ELM} is the total ELM energy for each pulse; E_{QUENCH} is the energy necessary for perfect quenching of recombination in the recombining region. According to Table I, we have four categories. In the first case

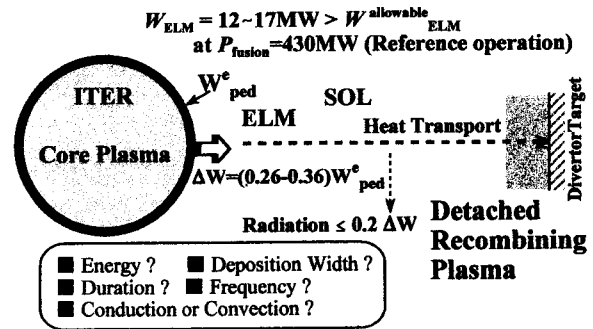


Fig. 2 ELM energy transport across the separatrix, through SOL and detached plasma, finally onto the divertor target plate.

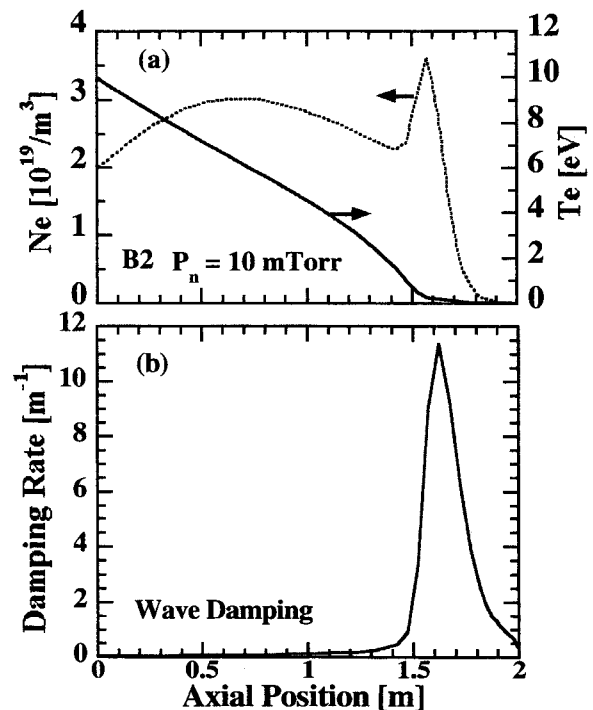


Fig. 3 (a) Field-aligned structure of detached plasma obtained by B2 fluid simulation and (b) spatial profile of wave damping rate.

corresponding to top-left cell, we have a partial quenching of EIR due to an insufficient energy, followed by a convection of upstream warm plasma after ELM event due to short pulse duration compared with τ_{CONV} , and finally a slow recovery of EIR. This would be the case in the present experiment. We will come back again to this categorization after having explained the main results.

3.4 Structural Dynamics of Divertor Plasma

In the following, a structural dynamics of detached

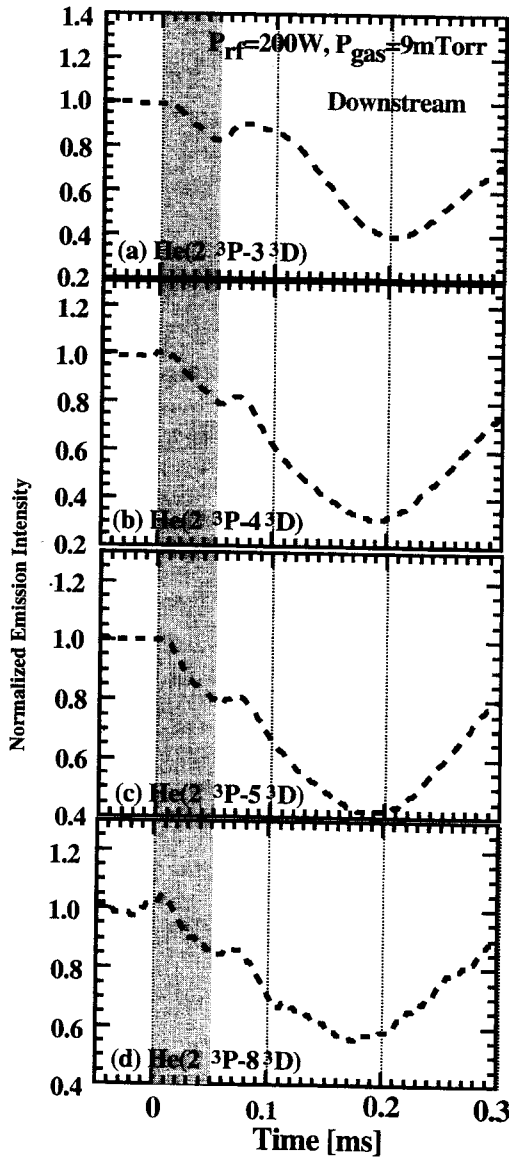


Fig. 4 Partial quenching of recombination and apparent "reheating" in detached plasma, viewed through He Balmer series emissions.

recombining plasma is discussed. Figure 4 shows some responses of He Balmer series emissions $\text{He}(2^3\text{P}-n^3\text{D})$ to the heat pulse with τ_{ELM} of 50 μs and P_{RF} of 200 W at the He gas pressure P_{He} of 9 mtorr, where a well detached He plasma is formed without heat pulse. Careful look at the time evolutions of Balmer series emissions suggests an apparent temporal development as follows: During the heat pulse the intensities mainly determined by recombining component go down indicating a weakening of recombination. They retain the level or tend to come back to the original level for a while. However, large reductions follow, having minimums at $t = 0.18 \sim 2.20$ ms. It seemed to us that

Table I Classification of ELM.

	$E_{ELM} < E_{Quench}$ (Partial Quenching of EIR)	$E_{ELM} > E_{Quench}$ (Perfect Quenching of EIR)
$\tau_{ELM} < \tau_{Conv}$	<ul style="list-style-type: none"> • Convection of upstream warm plasma after ELM • Slow recovery of EIR 	<ul style="list-style-type: none"> • Heat conduction of ELM energy direct to the target during pulse • Complete transition from recombining to ionizing • followed by slow convection after pulse • Recovery of EIR (Recombining)
$\tau_{ELM} > \tau_{Conv}$	<ul style="list-style-type: none"> • Convection of upstream warm plasma during ELM • EIR recovery starts after ELM 	<ul style="list-style-type: none"> • Heat conduction of ELM & SOL energy direct to the target during pulse • Complete transition from recombining to ionizing • continued by warm plasma convection after the pulse • Recovery of EIR (Recombining)

* Rydberg atoms play a role just at the beginning of heat pulse

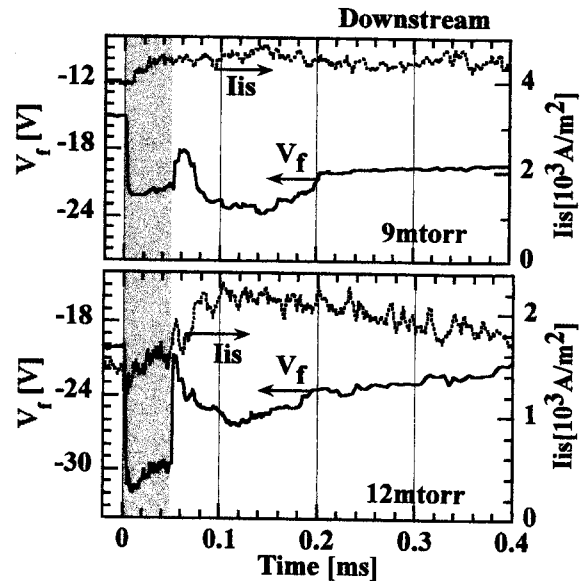


Fig. 5 Response of ion saturation current and floating potential detected with Langmuir probe to the heat pulse.

such great reductions come from a kind of plasma heating, which we call "reheating" phenomenon. "Reheating" is also detected in somewhat different ways by the floating potential V_f measurement with a Langmuir probe as shown in Fig. 5. A drop of V_f usually means a heating of plasma or an appearance of energetic electrons at this probe location. The minimums of V_f appear at $t = 0.12 \sim 0.15$ ms, that is, $50 \sim 80 \mu\text{s}$ earlier than those of line emissions. A real "reheating" is very difficult to be explained by, for example, a long confinement of hot electrons or a transport of heated plasma along the B field. Finally, we found that the upstream warm plasma flows into the recombining region to compensate a partial quenching of plasma recombination due to heat pulse. The time evolutions of V_f and emission intensities are different because the former is determined by the balance of ion and electron flux to the probe, and the latter is done by the balance of ionizing and recombining components in CR processes. The idea standing for the transport of upstream plasma

is well represented by V_f measurements at several locations along the field line, as shown in Fig. 6, in which the timings of V_f minimum is really delayed as the location approaches the target. Figure 5 also shows a slow increase in ion flux to the probe, indicating a plasma flow into the recombining region so that the mystery of "reheating" is now supposed to be resolved. After the "reheating", a slow recovery of plasma recombination takes place in the time scale of 0.5 to 1.0 ms.

Figure 7 shows a schematic of structural dynamics according to the heat pulse. We note that a sharp drop of V_f during rf heat pulse comes from the arrival of supra-thermal electrons to the recombining region where the plasma density is so low that their influence appear drastically because their flux could be comparable to or greater than the ion flux.

3.5 Response to Heat Pulse Train

A series of heat pulse with each duration of only 20 μs and the rf power of 200 W, and at a rather fast repetition of 10 kHz was injected into the originally detached recombining plasma. The responses of emission intensities, ion flux to the probe and floating potential are shown in Figs. 8, 9 and 10, respectively. We note that the probes were moving during the pulse injection (6 mm/4 ms). That is the reason why the ion flux and floating potential without rf are apparently changing in time. Even a short pulse destroys gradually the plasma recombination, introducing the upstream warm plasma into the downstream recombining region, increasing the ion flux and decreasing V_f there although there are only little effects on the upstream plasma. During the whole pulse train, the ion flux and V_f have quasi steady values in about 1.0 ms. After the pulse train the recovery of them takes a time of 0.4 ~ 0.5 ms. The

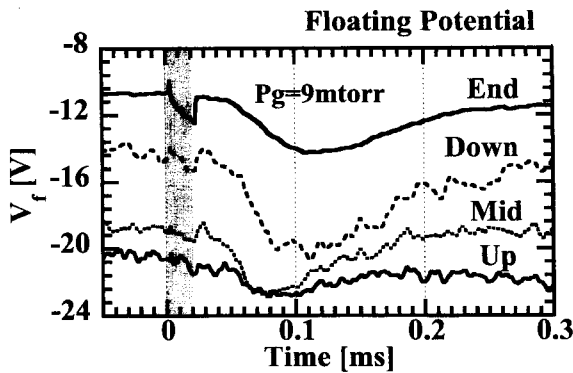


Fig. 6 Transport of upstream warm plasma into the recombining region to compensate the partial quenching.

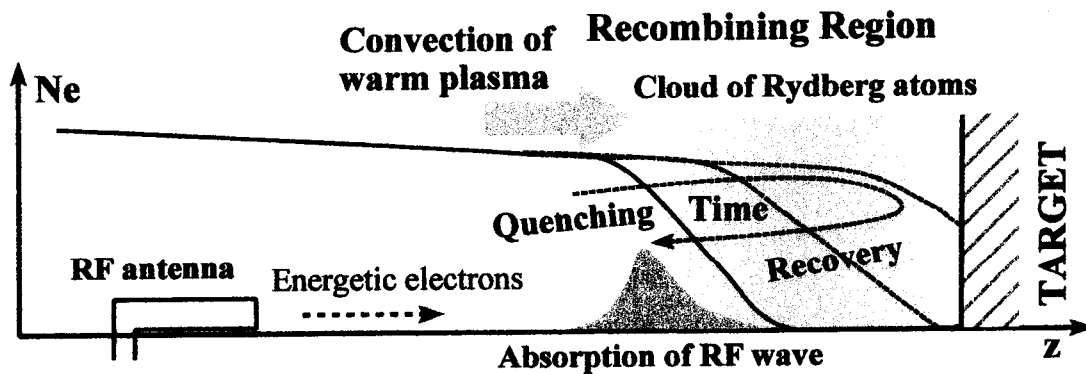


Fig. 7 Structural dynamics of detached plasma along the magnetic field when the heat pulse is injected.

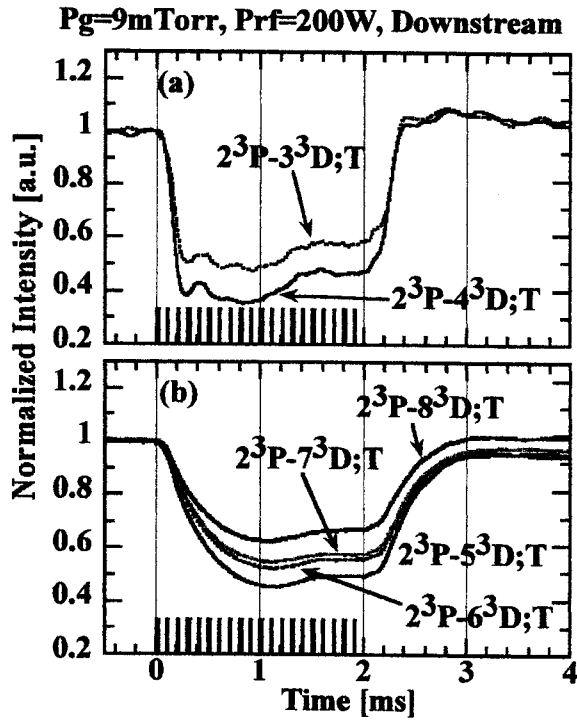


Fig. 8 Responses of He Balmer series emissions to the heat pulse train.

emission intensities from low excited levels ($n = 3$ and 4) have a relatively short time constant of $0.2 \sim 0.3$ ms as shown in Fig. 8(a), while those with high excited levels ($n = 5$ through 8) shown in Fig. 8(b) have a long characteristic time of about 0.6 ms. From the atomic physics point of view, the population on the low quantum principal numbers make a quick transition between recombining and ionizing, while those on highly excited levels are influenced more by the recombining component during an initial inflow of upstream warm plasmas. Slow recovery of recombination after the pulse train comes from slow cooling and recombination rates.

3.6 Other Dynamic Behaviors

A fairly strong heat pulse with $P_{rf} = 2$ kW and the pulse width of 0.5 ms makes a transition from recombining to ionizing during the pulse and then a back-transition from ionizing to recombining. These transitions are characterized by the so called negatively peaked double inverse ELM observed in tokamaks with divertor [20,21]. The physical origin was explained with

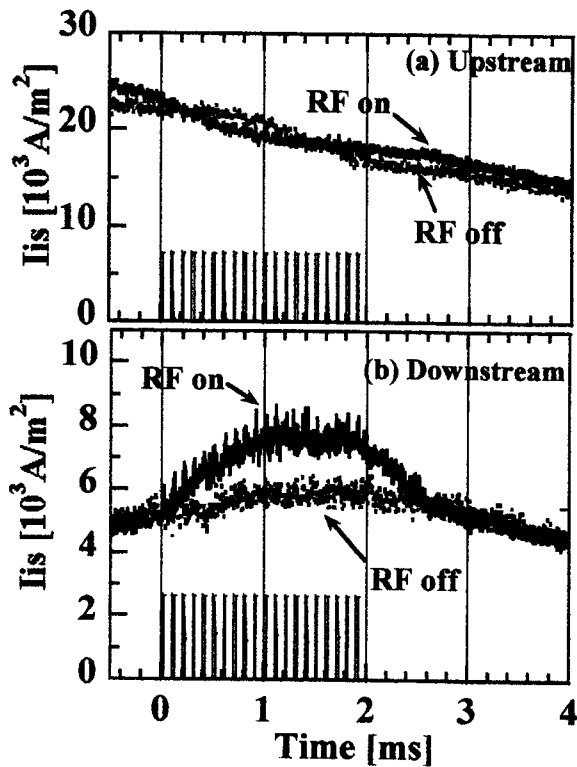


Fig. 9 Responses of ion current to the heat pulse train.

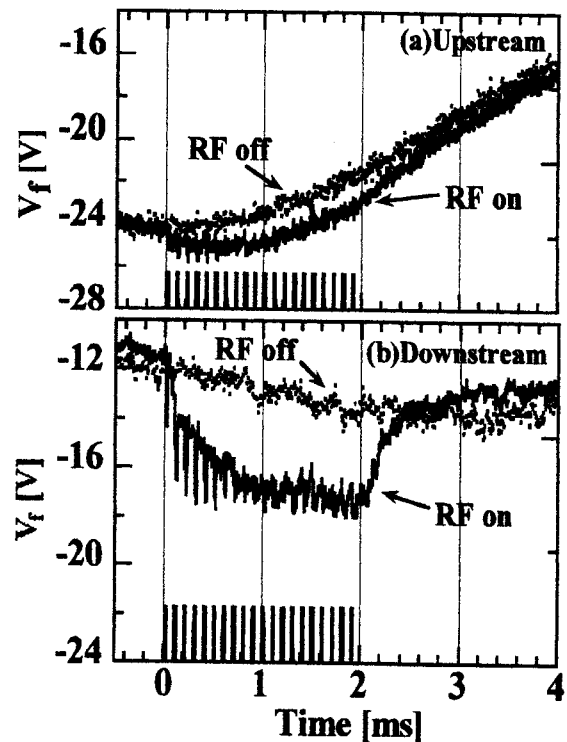


Fig. 10 Responses of floating potential of Langmuir probe to the heat pulse train.

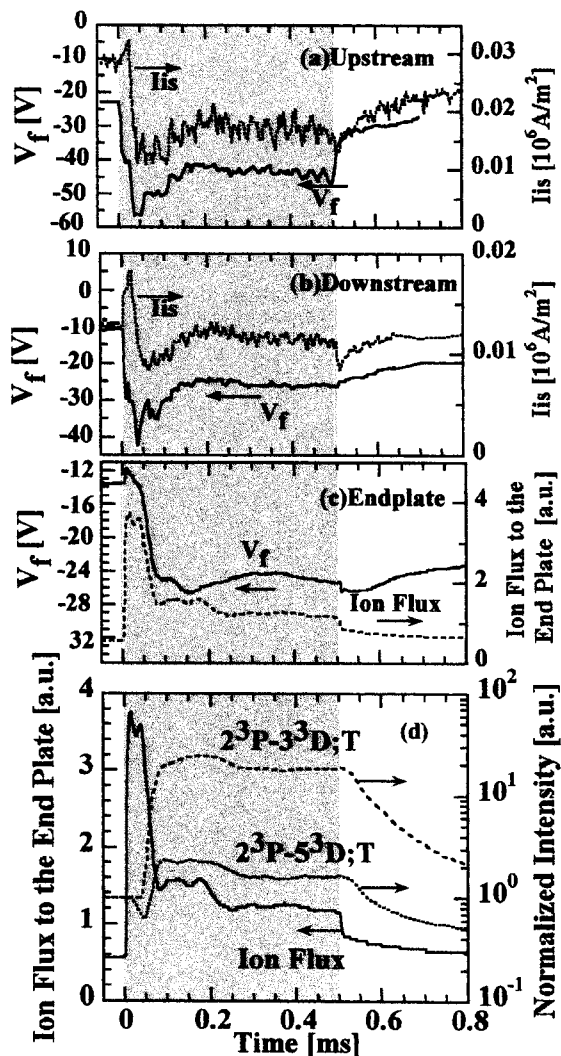


Fig. 11 Dynamic behaviors of ion currents and floating potential at the upstream, downstream and the end plate. He Balmer series emissions at downstream are also shown.

a CR model [12]. Such an ELM corresponds to the bottom-right cell of Table I. Under the same heat pulse condition, we observed that the ion flux to the target plate increased very quickly to be about seven times as large as the value before the heat pulse as shown in Figs. 11(c) and (d). The great increase in the ion flux lasts for only 0.06 ms. In this interval the emission intensity of He ($2^3P-5^3D:T$) line becomes weak or the emission He ($2^3P-3^3D:T$) is quiet first and then increases at $t = 0.06$ ms. Some modest increase in ion flux to the probe is observed at upstream as well as downstream as shown in Figs. 11(a) and (b). After $t = 0.1$ ms, the time evolution of these emission intensities and the ion flux

to the target show similar behaviors, which means that the electron impact excitation and ionization from the ground state are increased due to the energetic electrons produced by the rf heating. The floating voltage also starts to drop at $t = 0.06$ ms, see Fig. 11(c). The prompt increase of the ion flux at the beginning of rf pulse, however, can not be explained by the electron impact excitation from the ground state. A strong candidate for possible explanation is that highly excited Rydberg atoms produced by EIR are ionized by the energetic electrons because the ionization cross section of He atoms in highly excited levels was found to be quite large. Such Rydberg atoms play an important role in the net recombination, which could be related to the rapid increase of the ion flux to the target, a negative spike [17,18] or quiet behavior in the emission intensities and a delayed drop in V_f .

4. Conclusion

We have performed comprehensive investigation on the static as well as dynamic behaviors in detached recombining plasmas in the linear divertor plasma simulator, NAGDIS-II. For the stationary plasma detachment, contribution of MAR and EIR to the plasma detachment and a EIR-MAR transition were introduced by showing the key references.

We focus on the dynamic behaviors of detached recombining plasmas under the ELM-like heat pulse irradiation. Structural dynamics have been discussed basing on the experimental observations in terms of quenching of plasma recombination, compensating flow of upstream warm plasma into the recombining region, and recovery of recombination. Dynamic behaviors associated by the transition between recombining and ionizing plasmas was also identified. Heat pulses are categorized due to the heat pulse duration and the total pulse energy, in which several characteristic time scales and energies are defined. The role of highly excited Rydberg atoms generated by plasma recombination was discussed under the presence of energetic electrons due to heat pulse in relation to the dynamic behaviors of the ion flux to the target and its floating potential. These fundamental research would contribute the understanding of real ELM behaviors in fusion devices.

References

- [1] ITER Physics Expert Group on Divertor *et al.*, Nucl. Fusion **39**, 2391 (1999).
- [2] N. Ohno, S. Mori, N. Ezumi, M. Takagi, S.

- Takamura and H. Suzuki, *Contrib. Plasma Phys.* **36**, 339 (1996).
- [3] N. Ezumi, S. Mori, N. Ohno, M. Takagi, S. Takamura, H. Suzuki and J. Park, *J. Nucl. Mater.* **241-243**, 349 (1997).
- [4] D. Nishijima, N. Ezumi, K. Aoki, N. Ohno and S. Takamura, *Contrib. Plasma Phys.* **38**, 55 (1998).
- [5] N. Ezumi, N. Ohno, K. Aoki, D. Nishijima and S. Takamura, *Contrib. Plasma Phys.* **38**, 31 (1998).
- [6] N. Ohno, N. Ezumi, S. Takamura, S.I. Krasheninnikov and A. Yu Pigarov, *Phys. Rev. Lett.* **81**, 818 (1998).
- [7] N. Ohno, N. Ezumi, D. Nishijima and S. Takamura, *Czech. J. Phys.* **48**, 127 (1998).
- [8] D. Nishijima, N. Ezumi, H. Kojima, N. Ohno, S. Takamura, S.I. Krasheninnikov and A.Yu Pigarov, *J. Nucl. Mater.* **266-269**, 1161 (1999).
- [9] N. Ohno, M. Tanaka, N. Ezumi, D. Nishijima, S. Takamura, S.I. Krasheninnikov, A.Yu Pigarov and J. Park, *Phys. Plasmas* **6**, 2486 (1999).
- [10] N. Ezumi, D. Nishijima, H. Kojima, N. Ohno, S. Takamura, S.I. Krasheninnikov and A.Yu Pigarov, *J. Nucl. Mater.* **266-269**, 237 (1999).
- [11] D. Nishijima, U. Wenzel, M. Motoyama, N. Ohno, S. Takamura and S.I. Krasheninnikov, *J. Nucl. Mater.* **290-293**, 688 (2001).
- [12] N. Ohno, D. Nishijima, M. Motoyama, N. Hattori, Y. Uesugi, S. Takamura, U. Wenzel, *J. Plasma Fusion Res. SERIES* **3**, 202 (2000).
- [13] Y. Uesugi, N. Hattori, D. Nishijima, N. Ohno and S. Takamura, *J. Nucl. Mater.* **290-293**, 1134 (2001).
- [14] S.I. Krasheninnikov *et al.*, *Phys. Lett. A* **214**, 285 (1996).
- [15] D.E. Post, *J. Nucl. Mater.* **220-222**, 143 (1995).
- [16] A.Yu Pigarov, *et al.*, *Phys. Lett. A* **222**, 251 (1996).
- [17] S. Takamura, N. Ohno, Y. Uesugi, D. Nishijima, M. Motoyama, N. Hattori, H. Arakawa, N. Ezumi, S. Krasheninnikov, A. Pigarov and U. Wenzel, *Proc. 18th IAEA Fusion Energy Conf. Sorrento, Italy, 4 to 10 October, 2000, IAEA-CN-77/EXP4/29*.
- [18] N. Ohno, D. Nishijima, S. Takamura, Y. Uesugi, M. Motoyama, N. Hattori, H. Arakawa, N. Ezumi, S. Krasheninnikov, A. Pigarov, U. Wenzel, *Nucl. Fusion* **41**, 1055 (2001).
- [19] A. Loarte *et al.*, "Predicted ELM Energy Loss and Power Loading in ITER-FEAT", *Proc. 18th IAEA Fusion Energy Conf. Sorrento, Italy, 4 to 10 October, 2000, IAEA-CN-77/ITER/2-ITERP/11*.
- [20] A. Loarte, R.D. Monk *et al.*, *Nucl. Fusion* **38**, 331 (1998).
- [21] U. Wenzel *et al.*, *J. Nucl. Mater.* **266-269**, 1252 (1999).